Relative Pose Estimation and Fusion of 2D Spectral and 3D Lidar Images[*]

Zoltan Kato[1] and Levente Tamas[2]

[1] Institute of Informatics, University of Szeged, P.O. Box 652, H-6701 Szeged, Hungary. `kato@inf.u-szeged.hu`
[2] Technical University of Cluj-Napoca, Robotics Research Group, Dorobantilor st. 73, 400609, Romania. `levente.tamas@aut.utcluj.ro`

Abstract. This paper presents a unified approach for the relative pose estimation of a spectral camera - 3D Lidar pair without the use of any special calibration pattern or explicit point correspondence. The method works without specific setup and calibration targets, using only a pair of 2D-3D data. Pose estimation is formulated as a 2D-3D nonlinear shape registration task which is solved without point correspondences or complex similarity metrics. The registration is then traced back to the solution of a non-linear system of equations which directly provides the calibration parameters between the bases of the two sensors. The method has been extended both for perspective and omnidirectional central cameras and was tested on a large set of synthetic lidar-camera image pairs as well as on real data acquired in outdoor environment.

1 Introduction

In the past years there was a considerable research effort invested in the fusion of heterogeneous image data acquired from 2D and 3D sensors [24]. The need for fusing such sensory data is common to various research fields including remote sensing [17], medical image processing [20,3,12], mobile robotic applications [6], urban autonomous driving [5], geodesic information fusion [27], cultural heritage documentation [1], or entertainment related commercial depth cameras[2]. One of the most challenging issues is the fusion of 2D RGB imagery with other 3D range sensing modalities (*e.g.* Lidar) which can be formulated as a camera calibration task. Internal calibration refers to the self parameters of the camera, while external parameters describe the *pose* of the camera with respect to a world coordinate frame. The problem becomes more difficult, when the RGB image is recorded with a non-conventional camera, such as central catadioptric

or dioptric (*e.g.* fish-eye) panoramic cameras. This paper focuses on the extrinsic parameter estimation for a range-camera sensor pair, where the 3D rigid motion between the two camera coordinate systems is determined. Due to the different functionality of the ranger (*e.g.* lidar) and central camera, the calibration is often performed manually, or by considering special assumptions like artificial markers on images, or establishing point matches. These procedures tend to be laborious and time consuming, especially when calibration has to be done more than once during data acquisition. In real life applications, however, it is often desirable to have a flexible one step calibration without such prerequisites.

Based on our earlier works [26,25], this paper presents a region based calibration framework for spectral 2D central cameras and 3D lidar. Instead of establishing point matches or relying on artificial markers or recorded intensity values, we propose a relative pose estimation algorithm which works with segmented planar patches. Since segmentation is required anyway in many real-life image analysis tasks, such regions may be available or straightforward to detect. The main advantage of the proposed method is the use of regions instead of point correspondence and a generic problem formulation which allows to treat several types of cameras in the same framework. Basically, we reformulate pose estimation as a shape alignment problem, which is accomplished by solving a system of nonlinear equations. The method has been quantitatively evaluated on a large synthetic dataset both for perspective [26] and omnidirectional [25] cameras, and it proved to be robust and efficient in real-life situations.

1.1   Related work

There are various techniques applied for camera calibration, *e.g.* point or line correspondence finding [13], intensity image based correlation [19], use of specific artificial land-marks [8] or mutual information extraction and parameter optimization[11]. The extrinsic calibration of 3D lidar and low resolution color camera was first addressed in [28] which generalized the algorithm proposed in [29]. This method is based on manual point feature selection from both sensory data and it assumes a valid camera intrinsic model for calibration. A similar manual point feature correspondence based approach is proposed in [21]. There are also extensions to the simultaneous intrinsic-extrinsic calibration presented in the work [16] which used the intensity information from lidar to find correspondences between the 2D-3D domains. Other works are based on the fusion of IMU or GPS information in the process of 2D-3D calibration [18], mainly in the initialization phase of the calibration [27]. Recently there has been an increasing interest in various calibration problem setups ranging from high-resolution spatial data registration [13] to low-resolution, high frame rate depth commercial cameras such as Kinect [9], or in the online calibration during different measurements in time such as in case of a traveling mobile robot [19].

The most commonly used non-perspective central camera systems, especially for robotics and autonomous driving, are using omnidirectional (or panoramic) lenses. The geometric formulation of such systems were extensively studied [15,22,23].

The internal calibration of such cameras depends on these geometric models. Although different calibration methods and toolboxes exist [22,10,14] this problem is by far not trivial and is still in focus [23]. While internal calibration can be solved in a controlled environment, using special calibration patterns, pose estimation must rely on the actual images taken in a real environment. There are popular methods dealing with point correspondence estimation such as [22] or other fiducial marker images suggested in [10], which may be cumbersome to use in real life situations. This is especially true in a multimodal setting, when omnidirectional images need to be combined with other non-conventional sensors like lidar scans providing only range data. The Lidar-omnidirectional camera calibration problem was analyzed from different perspectives: in [21], the calibration is performed in natural scenes, however the point correspondences between the 2D-3D images are selected in a semi-supervised manner. The method in [16] tackles calibration as an observability problem using a (planar) fiducial marker as calibration pattern. In [19], a fully automatic method is proposed based on mutual information (MI) between the intensity information from the depth sensor and the omnidirectional camera. Also based on MI, [27] performs the calibration using particle filtering. However, these methods require a range data with recorded intensity values, which is not always possible and often challenged by real-life lighting conditions.

2 Region-based calibration framework

Consider a lidar camera with a 3D coordinate system having its origin $\mathbf{O}$ in the rotation center of the laser sensor, x and y axes pointing to the right and down, respectively, while z is pointing away from the sensor. Setting the world coordinate system to the lidar's coordinate frame, we can always express a 3D lidar point $\mathbf{X}$ with its homogeneous world coordinates $\mathbf{X} = (X_1, X_2, X_3, 1)^T$.

A classical perspective camera sees the same world point $\mathbf{X}$ as a homogeneous point $\mathbf{x} = (x_1, x_2, 1)^T$ in the image plain obtained by a perspective projection $\mathbf{P}$:

$$\mathbf{x} = \mathbf{PX} = \mathbf{KR}[\mathbf{I}|\mathbf{t}]\mathbf{X}, \tag{1}$$

where $\mathbf{P}$ is the 3×4 camera matrix, which can be factored into the well known $\mathbf{P} = \mathbf{KR}[\mathbf{I}|\mathbf{t}]$ form, where $\mathbf{I}$ is the identity matrix, $\mathbf{K}$ is the 3×3 upper triangular *calibration* matrix containing the camera intrinsic parameters, while $\mathbf{R}$ and $\mathbf{t}$ are the rotation and translation, respectively, aligning the camera frame with the world coordinate frame. A classical solution of the calibration problem is to establish a set of 2D-3D point matches using a special calibration target [9,16], and then solve for $\mathbf{P}$ via a system of equation based on (1) or the minimization of some error function. When a calibration target is not available, then solutions typically assume that the lidar points contain also the laser reflectivity value (interpreted as a gray-value), which can be used for intensity-based matching or registration [21,13].

However, in many practical applications (*e.g.* infield mobile robot), it is not possible to use a calibration target and most lidar sensors will only record depth

information. Furthermore, lidar and camera images might be taken at differ-
ent times and they need to be fused later based solely on the image content.
Therefore the question naturally arises: what can be done when neither a spe-
cial target nor point correspondences are available? Herein, we present a solution
for such challenging situations. In particular, we will show that by identifying a
single planar region both in the lidar and camera image, the extrinsic calibra-
tion can be solved. When two such non-coplanar regions are available then the
full calibration can be solved. Of course, these are just the necessary minimal
configurations. The more such regions are available, a more stable calibration is
obtained.

Hereafter, we will focus only on the relative pose $(\mathbf{R}, \mathbf{t})$ estimation, hence
we assume that for perspective cameras $\mathbf{K}$ is known. As for omnidirectional
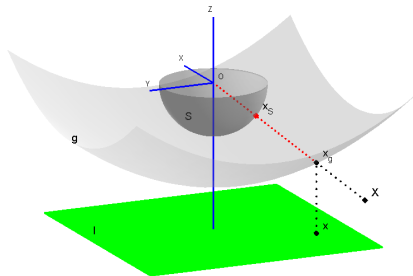cameras, the intrinsic parameters and relative pose is discussed below.

Fig. 1. Omnidirectional camera model

2.1 Omnidirectional camera model

A unified model for central omnidirectional cameras was proposed by Geyer
and Daniilidis [7], which represents central panoramic cameras as a projection
onto the surface of a unit sphere. This formalism has been adopted and models
for the internal projection function have been proposed by Micusik [15] and
subsequently by Scaramuzza [22] who derived a general polynomial form of the
internal projection valid for any type of omnidirectional camera. In this work,
we will use the latter representation.

Let us first see the relationship between a point $\mathbf{x}$ in the omnidirectional
image $\mathcal{I}$ and its representation on the unit sphere $\mathcal{S}$ (see Fig. 1). Note that
only the half sphere on the image plane side is actually used, as the other half
is not visible from image points. Following [22], we assume that the camera
coordinate system is in $\mathcal{S}$, the origin (which is also the center of the sphere)
is the projection center of the camera and the z axis is the optical axis of the
camera which intersects the image plane in the *principal point*. To represent
the nonlinear (but symmetric) distortion of central omnidirectional optics, [22]

places a surface g between the image plane and the unit sphere $\mathcal{S}$, which is rotationally symmetric around z. Herein, as suggested by [22], we will use a fourth order polynomial $g(\|\mathbf{x}\|) = a_0 + a_2\|\mathbf{x}\|^2 + a_3\|\mathbf{x}\|^3 + a_4\|\mathbf{x}\|^4$ which has 4 parameters representing the internal parameters (a_0, a_2, a_3, a_4) of the camera. The bijective mapping $\Phi : \mathcal{I} \to \mathcal{S}$ is composed of 1) lifting the image point $\mathbf{x} \in \mathcal{I}$ onto the g surface by an orthographic projection

$$\mathbf{x}_g = \begin{bmatrix} \mathbf{x} \\ a_0 + a_2\|\mathbf{x}\|^2 + a_3\|\mathbf{x}\|^3 + a_4\|\mathbf{x}\|^4 \end{bmatrix} \tag{2}$$

and then 2) centrally projecting the lifted point $\mathbf{x}_g$ onto the surface of the unit sphere $\mathcal{S}$:

$$\mathbf{x}_\mathcal{S} = \Phi(\mathbf{x}) = \frac{\mathbf{x}_g}{\|\mathbf{x}_g\|} \tag{3}$$

Thus the omnidirectional camera projection is fully described by means of unit vectors $\mathbf{x}_\mathcal{S}$ in the half space of $\mathbb{R}^3$.

The projection of a 3D world point $\mathbf{X} \in \mathbb{R}^3$ onto $\mathcal{S}$ is basically a traditional central projection onto $\mathcal{S}$ taking into account the extrinsic pose parameters ($\mathbf{R}$, $\mathbf{t}$) acting between the camera (represented by $\mathcal{S}$) and the world coordinate frame. Thus for a world point $\mathbf{X}$ and its image $\mathbf{x}$ in the omnidirectional camera, the following holds on the surface of $\mathcal{S}$:

$$\Phi(\mathbf{x}) = \mathbf{x}_\mathcal{S} = \Psi(\mathbf{X}) = \frac{\mathbf{R}\mathbf{X} + \mathbf{t}}{\|\mathbf{R}\mathbf{X} + \mathbf{t}\|} \tag{4}$$

2.2   Pose Estimation

Our solution for the relative pose is based on the 2D shape registration approach of Domokos *et al.* [4], where the alignment of non-linear shape deformations are recovered via the solution of a special system of equations. Here, however, the calibration problem yields a 2D-3D registration problem in case of a perspective camera and a restricted 3D-3D registration problem on the spherical surface for omnidirectional cameras. These cases thus require a different technique to construct the system of equations.

2.3   Relative pose of perspective cameras

Since correspondences are not available, (1) cannot be used directly. However, individual point matches can be integrated out yielding the following integral equation:

$$\int_\mathcal{D} \mathbf{x}d\mathbf{x} = \int_{\mathbf{P}\mathcal{F}} \mathbf{z}d\mathbf{z}, \tag{5}$$

where $\mathcal{D}$ corresponds to the region visible in the *camera* image and $\mathbf{P}\mathcal{F}$ is the image of the *lidar region* projected by the camera matrix $\mathbf{P}$. The above equation corresponds to a system of 2 equations only, which is clearly not sufficient to solve for all parameters of the camera matrix $\mathbf{P}$. Therefor we adopt the general

mechanism proposed in [4] to construct new equations. Indeed, (1) remains valid when a function $\omega : \mathbb{R}^2 \rightarrow \mathbb{R}$ is acting on both sides of the equation

$$\omega(\mathbf{x}) = \omega(\mathbf{PX}), \tag{6}$$

and the integral equation of (5) becomes [26]

$$\int_{\mathcal{D}} \omega(\mathbf{x}) d\mathbf{x} = \int_{\mathbf{P}\mathcal{F}} \omega(\mathbf{z}) d\mathbf{z}. \tag{7}$$

Adopting a set of nonlinear functions $\{\omega_i\}_{i=1}^{\ell}$, each ω_i generates a new equation yielding a system of ℓ independent equations. Hence we are able to generate sufficiently many equations. The parameters of the camera matrix $\mathbf{P}$ are then simply obtained as the solution of the nonlinear system of equations (7). In practice, an overdetermined system is constructed, which is then solved by minimizing the algebraic error in the *least squares sense* via a standard *Levenberg-Marquardt* algorithm.

Note that computing the integral on the right hand side of (7) involves the actual execution of the camera projection $\mathbf{P}$ on $\mathcal{F}$, which might be computationally unfavorable. However, choosing power functions for ω_i [26]:

$$\omega_i(\mathbf{x}) = x_1^{n_i} x_2^{m_i}, \quad n_i \leq 3 \text{ and } m_i \leq 3 \tag{8}$$

and using a triangular mesh representation $\mathcal{F}^\triangle$ of the lidar region $\mathcal{F}$, we can adopt an efficient computational scheme. First, let us note that this particular choice of ω_i yields the 2D geometric moments of the projected lidar region $\mathbf{P}\mathcal{F}$. Furthermore, due to the triangular mesh representation of $\mathcal{F}$, we can rewrite the integral adopting ω_i from (8) as [26]

$$\int_{\mathcal{D}} x_1^{n_i} x_2^{m_i} d\mathbf{x} \quad = \quad \int_{\mathbf{P}\mathcal{F}} z_1^{n_i} z_2^{m_i} d\mathbf{z} \quad \approx \quad \sum_{\forall \triangle \in \mathcal{F}^\triangle} \int_{\triangle} z_1^{n_i} z_2^{m_i} d\mathbf{z}. \tag{9}$$

The latter approximation is due to the approximation of $\mathcal{F}$ by the discrete mesh $\mathcal{F}^\triangle$. The integrals over the triangles are various geometric moments which can be computed using efficient recursive formulas [26].

2.4 Relative pose of spherical cameras

For omnidirectional cameras, we have to work on the surface of the unit sphere as it provides a representation independent of the camera internal parameters. Therefore the system of equation has the following form [25]:

$$\iint_{\mathcal{D}_\mathcal{S}} \omega(\mathbf{x}_\mathcal{S}) \, \mathrm{d}\mathcal{D}_\mathcal{S} = \iint_{\mathcal{F}_\mathcal{S}} \omega(\mathbf{z}_\mathcal{S}) \, \mathrm{d}\mathcal{F}_\mathcal{S} \tag{10}$$

$\mathcal{D}_\mathcal{S}$ and $\mathcal{F}_\mathcal{S}$ denote the surface patches on $\mathcal{S}$ corresponding to the omni and lidar planar regions $\mathcal{D}$ and $\mathcal{F}$, respectively. To get an explicit formula for the above

integrals, the surface patches $\mathcal{D}_\mathcal{S}$ and $\mathcal{F}_\mathcal{S}$ can be naturally parameterized via Φ and Ψ over the planar regions $\mathcal{D}$ and $\mathcal{F}$. Without loss of generality, we can assume that the third coordinate of $\mathbf{X} \in \mathcal{F}$ is 0, hence $\mathcal{D} \subset \mathbb{R}^2$, $\mathcal{F} \subset \mathbb{R}^2$; and $\forall \mathbf{x}_\mathcal{S} \in \mathcal{D}_\mathcal{S} : \mathbf{x}_\mathcal{S} = \Phi(\mathbf{x}), \mathbf{x} \in \mathcal{D}$ as well as $\forall \mathbf{z}_\mathcal{S} \in \mathcal{F}_\mathcal{S} : \mathbf{z}_\mathcal{S} = \Psi(\mathbf{X}), \mathbf{X} \in \mathcal{F}$ yielding the following form of (10) [25]:

$$\iint_\mathcal{D} \omega(\Phi(\mathbf{x})) \left\| \frac{\partial \Phi}{\partial x_1} \times \frac{\partial \Phi}{\partial x_2} \right\| \mathrm{d}x_1 \, \mathrm{d}x_2 = \iint_\mathcal{F} \omega(\Psi(\mathbf{X})) \left\| \frac{\partial \Psi}{\partial X_1} \times \frac{\partial \Psi}{\partial X_2} \right\| \mathrm{d}X_1 \, \mathrm{d}X_2$$

(11)

where the magnitude of the cross product of the partial derivatives is known as the surface element. Adopting a set of nonlinear functions $\{\omega_i\}_{i=1}^\ell$, each ω_i generates a new equation yielding a system of ℓ independent equations. Although arbitrary ω_i functions could be used, power functions are computationally favorable [4,26] as these can be computed in a recursive manner:

$$\omega_i(\mathbf{x}_\mathcal{S}) = x_1^{l_i} x_2^{m_i} x_3^{n_i}, \text{ with } 0 \leq l_i, m_i, n_i \leq 2 \text{ and } l_i + m_i + n_i \leq 3 \qquad (12)$$

2.5   Algorithm summary

The summary of the numerical implementation of the proposed method is presented in Algorithm 1. Note that normalization is critical in the perspective case to ensure a numerically stable solution (see [4,26] for details). In the omnidirectional case, we use the coordinates on the spherical surface which are already normalized as $\mathcal{S}$ is a unit sphere.

Algorithm 1 The proposed calibration algorithm

Input: 3D point cloud and 2D binary image representing the same region, and the internal camera parameters (either $\mathbf{K}$ or (a_0, a_2, a_3, a_4)).
Output: Relative pose $(\mathbf{R}, \mathbf{t})$.
 1: For perspective cameras, normalize 3D points into the unit cube and the 2D points into the unit square centered in the origin. For omnidirectional cameras, project 3D points and 2D image pixels onto the surface of $\mathcal{S}$ using (3) and (4).
 2: Triangulate the region represented by the 3D point cloud.
 3: Construct the system of equations. For perspective cameras, use (9) with the polynomial ω_i functions of (8), whereas for omnidirectional cameras, use (11).
 4: Initialize the relative pose $(\mathbf{I}, \mathbf{0})$ for perspective cameras and follow the initialization procedure from [25] for omnidirectional cameras.
 5: Solve the nonlinear system of equations using the Levenberg-Marquardt algorithm
 6: Unnormalize the solution.

---

3   Discussion

In this paper a method for relative pose estimation of central cameras has been presented. The method is based on a point correspondence-less registration tech-
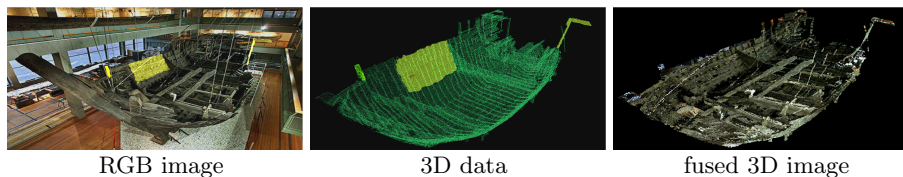
RGB image   3D data   fused 3D image

Fig. 2. Cultural heritage use case example with the *Bremen Cog*. Segmented planar regions are shown in yellow (best viewed in color).
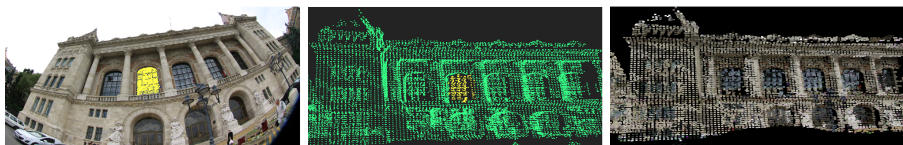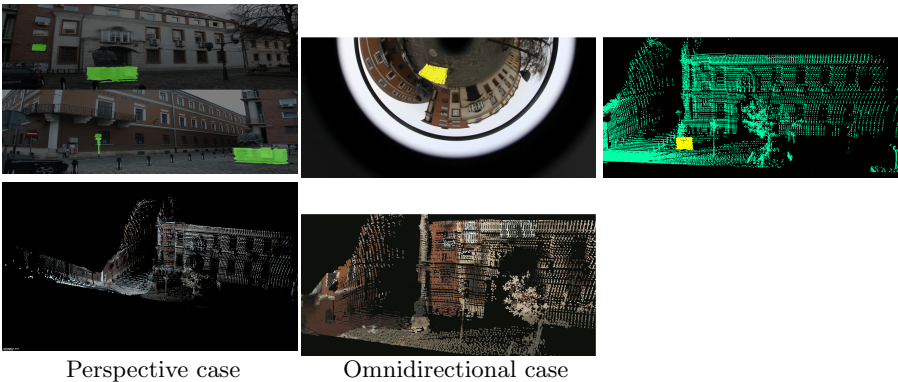

Fig. 3. Dioptric (fish eye) and lidar images with segmented area marked in yellow, and the fused images after pose estimation (best viewed in color)

nique, which allows reliable estimation of extrinsic camera parameters. The presented algorithms have been applied to various datasets. Three representative examples are shown in Fig. 2, Fig. 4, and Fig. 3. The perspective images in Fig. 2 and Fig. 4 were obtained with a commercial camera while the omnidirectional images were captured with a catadioptric lens in Fig. 4 and a fish-eye in Fig. 3, respectively. After the raw data acquisition, the segmentation was performed in both domains. Finally, the estimated transformation was used to fuse the depth and RGB data by reprojecting the point cloud on the image plane using the internal and external camera parameters, and thus obtaining the color for each point of the 3D point cloud. The method proved to be robust against segmentation errors, but a sufficiently large overlap between the regions is required for better results.

References

1. Boochs, F., Bentkowska-Kafel, A., Degrigny, C., Karaszewski, M., Karmacharya, A., Kato, Z., Picollo, M., Sitnik, R., Trémeau, A., Tsiafaki, D., et al.: Colour and space in cultural heritage: Key questions in 3d optical documentation of material culture for conservation, study and preservation. In: Digital Heritage. Progress in Cultural Heritaage: Documentation, Preservation, and Protection, pp. 11–24. Springer International Publishing (2014)
2. Bouaziz, S., Pauly, M.: Dynamic 2d/3d registration for the kinect. In: ACM SIG-GRAPH 2013 Courses. pp. 21:1–21:14. SIGGRAPH '13, ACM, New York, NY, USA (2013)
3. Cao, T., Zach, C., Modla, S., Czymmek, D.P.K., Niethammer, M.: Multi-modal registration for correlative microscopy using image analogies. Medical Image Analysis 18(6), 914 – 926 (2014), sparse Methods for Signal Reconstruction and Medical Image Analysis

Perspective case   Omnidirectional case

Fig. 4. Perspective, catadioptric and lidar images with segmented area marked in yellow, and the fused images after pose estimation (best viewed in color)

4. Domokos, C., Nemeth, J., Kato, Z.: Nonlinear Shape Registration without Correspondences. IEEE Transactions on Pattern Analysis and Machine Intelligence 34(5), 943–958 (2012)
5. Geiger, A., Lauer, M., Wojek, C., Stiller, C., Urtasun, R.: 3D Traffic Scene Understanding From Movable Platforms. IEEE Transactions on Pattern Analysis and Machine Intelligence 36(5), 1012–1025 (2014)
6. Geiger, A., Moosmann, F., Car, O., Schuster, B.: Automatic camera and range sensor calibration using a single shot. In: International Conference on Robotics and Automation. pp. 3936–3943. IEEE (2012)
7. Geyer, C., Daniilidis, K.: A unifying theory for central panoramic systems. In: European Conference on Computer Vision. pp. 445–462. Dublin, Ireland (June 2000)
8. Gong, X., Lin, Y., Liu, J.: Extrinsic calibration of a 3d lidar and a camera using a trihedron. Optics and Lasers in Engineering 51(4), 394 – 401 (2013)
9. Herrera C, D., Kannala, J., Heikkila, J.: Joint depth and color camera calibration with distortion correction. IEEE Transactions on Pattern Analysis and Machine Intelligence 34(10), 1–8 (2012)
10. Kannala, J., Brandt, S.S.: A Generic Camera Model and Calibration Method for Conventional, Wide-Angle, and Fish-Eye Lenses. IEEE Transactions on Pattern Analysis and Machine Intelligence 28(8), 1335–1340 (2006)
11. Li, Y., Ruichek, Y., Cappelle, C.: Optimal extrinsic calibration between a stereoscopic system and a lidar. Instrumentation and Measurement, IEEE Transactions on 62(8), 2258–2269 (2013)
12. Markelj, P., Tomaževič, D., Likar, B., Pernuš, F.: A review of 3d/2d registration methods for image-guided interventions. Medical Image Analysis 16(3), 642 – 661 (2012), computer Assisted Interventions
13. Mastin, A., Kepner, J., III, J.W.F.: Automatic registration of lidar and optical images of urban scenes. In: IEEE Computer Society Conference on Computer Vision and Pattern Recognition. pp. 2639–2646. IEEE, Miami, Florida, USA (June 2009)
14. Mei, C., Rives, P.: Single View Point Omnidirectional Camera Calibration from Planar Grids. In: International Conference on Robotics and Automation. pp. 3945–3950. Roma, Italy (April 2007)

15. Mičušík, B., Pajdla, T.: Para-catadioptric Camera Auto-calibration from Epipolar Geometry. In: Asian Conference on Computer Vision. vol. 2, pp. 748–753. Seoul, Korea South (January 2004)
16. Mirzaei, F.M., Kottas, D.G., Roumeliotis, S.I.: 3D LIDAR-camera intrinsic and extrinsic calibration: Identifiability and analytical least-squares-based initialization. International Journal of Robotics Research 31(4), 452–467 (2012)
17. Mishra, R., Zhang, Y.: A review of optical imagery and airborne lidar data registration methods. The Open Remote Sensing Journal 5, 54–63 (2012)
18. Nunez, P., Drews, P., Rocha, R., Dias, J.: Data fusion calibration for a 3d laser range finder and a camera using inertial data. In: European Conference on Mobile Robots. pp. 31—36. Dubrovnik, Croatia (September 2009)
19. Pandey, G., McBride, J.R., Savarese, S., Eustice, R.M.: Automatic Targetless Extrinsic Calibration of a 3D Lidar and Camera by Maximizing Mutual Information. In: AAAI National Conference on Artificial Intelligence. pp. 2053–2059. Toronto, Canada (July 2012)
20. Pluim, J., Maintz, J., Viergever, M.: Mutual-information-based registration of medical images: a survey. Medical Imaging, IEEE Transactions on 22(8), 986–1004 (2003)
21. Scaramuzza, D., Harati, A., Siegwart, R.: Extrinsic Self Calibration of a Camera and a 3D Laser Range Finder from Natural Scenes. In: International Conference on Intelligent Robots and Systems. pp. 4164–4169. San Diego, USA (October 2007)
22. Scaramuzza, D., Martinelli, A., Siegwart, R.: A Flexible Technique for Accurate Omnidirectional Camera Calibration and Structure from Motion. In: International Conference on Computer Vision Systems. pp. 45–51. Washington, USA (January 2006)
23. Schoenbein, M., Strauss, T., Geiger, A.: Calibrating and Centering Quasi-Central Catadioptric Cameras. In: International Conference on Robotics and Automation. pp. 1253–1256. Hong-Kong, China (June 2014)
24. Stamos, I.: Automated registration of 3d-range with 2d-color images: an overview. In: Information Sciences and Systems (CISS), 2010 44th Annual Conference on. pp. 1–6 (March 2010)
25. Tamas, L., Frohlich, R., Kato, Z.: Relative pose estimation and fusion of omnidirectional and lidar cameras. In: ECCV Workshop on Computer Vision for Road Scene Understanding and Autonomous Driving (ECCV-CVRSUAD). pp. 1–12. Lecture Notes in Computer Science, Zurich, Switzerland (September 2014)
26. Tamas, L., Kato, Z.: Targetless Calibration of a Lidar - Perspective Camera Pair. In: International Conference on Computer Vision, Bigdata3dcv Workshops. pp. 668–675. Sydney, Australia (December 2013)
27. Taylor, Z., Nieto, J.: A Mutual Information Approach to Automatic Calibration of Camera and Lidar in Natural Environments. In: Australian Conference on Robotics and Automation. pp. 3–8. Wellington, Australia (December 2012)
28. Unnikrishnan, R., Hebert, M.: Fast extrinsic calibration of a laser rangefinder to a camera. Tech. rep., Carnegie Mellon University (2005)
29. Zhang, Q.: Extrinsic calibration of a camera and laser range finder. In: International Conference on Intelligent Robots and Systems. pp. 2301 – 2306. IEEE, Sendai, Japan (September 2004)